

Yoderite, a mineral with essential ferric iron: Its lack of occurrence in the system MgO-Al₂O₃-SiO₂-H₂O

T. FOCKENBERG, W. SCHREYER

Institut für Mineralogie, Ruhr-Universität, D-4630 Bochum, Germany

ABSTRACT

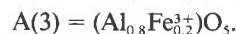
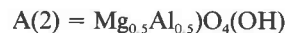
In experimental syntheses from gels, high yields of yoderite were obtained at high f_{O_2} only if the gels contained at least traces of Fe₂O₃ (as low as 0.0013 wt%). Synthetic yoderite has between 0.01 and 0.72 Fe³⁺ per formula unit (pfu) based on 19 O atoms, but only samples with about 0.2–0.4 Fe³⁺ pfu are stable at $P_H = 10$ kbar, 750 °C. Synthetic yoderite is monoclinic; all lattice parameters except β increase with increasing Fe³⁺ contents. In contrast to natural yoderite, the synthetic phase shows no indications of Mg,Al and Al,Fe³⁺ ordering at low temperature. Synthetic yoderite deviates from the ideal formula Mg₂(Al,Fe³⁺)₆Si₄O₁₈(OH)₂ in having higher (Al + Fe³⁺) but lower Mg and H⁺ contents; the higher Mg and H⁺ contents correlate with less Fe³⁺. Yoderite is stable under the f_{O_2} produced by the Mn₂O₃/MnO₂ and Mn₃O₄/Mn₂O₃ buffers. At lower f_{O_2} , yoderite forms initially from the Fe³⁺-bearing gel, but is subsequently partly replaced by staurolite-bearing assemblages. Additional experiments employing the seeding technique are necessary to determine stability relations of yoderite as a function of PTX and f_{O_2} with and without excess quartz.

INTRODUCTION

The mineral yoderite was discovered in 1959 by McKie at Mautia Hill, Tanzania, a locality within the Proterozoic Usagaran complex (Mruma and Basu, 1987). It occurs in a 5 m thick schist band as dark blue porphyroblasts up to 2 cm long together with kyanite, talc, quartz, and hematite. Based on the observation that kyanite and talc are separated from each other by yoderite with or without quartz, the reaction for the formation of yoderite was given by McKie (1959) as talc + kyanite = yoderite + quartz.

Using crystallographic data, Higgins et al. (1982) gave the ideal chemical formula of yoderite as Mg₂Al_{5.6}Fe_{0.4}³⁺Si₄O₁₈(OH)₂. This is close to the composition of the green yoderite variety of Mautia Hill (McKie and Bradshaw, 1966). If one replaces the trivalent Fe in this formula by more Al, hypothetical yoderite with Al as an end-member results; this can be represented in the pure system MgO-Al₂O₃-SiO₂-H₂O (MASH, Fig. 1). There the composition of yoderite lies on a line between kyanite and forsterite. The formula of yoderite can indeed be deduced theoretically from that of kyanite by the substitution Mg²⁺ + H⁺ = Al³⁺. There is also a structural kinship between yoderite and kyanite (Fleet and Megaw, 1962), which explains the topotactic overgrowth of yoderite on kyanite in the natural rock. Like kyanite, yoderite has chains of edge-sharing octahedra A(1) that extend parallel to its *b*-axis. In contrast to relations for kyanite, however, these chains are linked by two types of trigonal bipyramidal polyhedra, A(2) and A(3), occupied by the remaining large ions in five-coordination, and by isolated tetrahedra occupied ex-

clusively by Si. The site occupancies of the three large polyhedra in natural yoderite as reported by Higgins et al. (1982) are



PREVIOUS EXPERIMENTAL STUDIES

Schreyer and Yoder (1968), Schreyer and Seifert (1969), as well as Massonne and Schreyer (unpublished data, but see Schreyer, 1988) reported the synthesis of yoderite in the MASH system (Fig. 1). These syntheses were performed employing, in addition to pure chemicals, natural starting materials (andalusite from Brazil and natural yoderite as seeds) or a glass prepared using intermittent crushings in a steel mortar (see Schreyer and Schairer, 1961). Thus traces of Fe may have been present in all these experiments.

Schreyer and Yoder (1968) were able to synthesize yoderite in variable amounts over a considerable range of PT conditions. Their best yields were at 800 °C and 15 kbar with an estimated amount of yoderite of 98%, the remainder being talc. Because the exact oxide ratio of yoderite in the MASH system was not known at that time, starting materials with M:A:S ratios of 2:2:3, 4:5:7, and 2:3:4, all lying on the line between kyanite and forsterite, were used (Fig. 1). No chemical analyses of the synthetic yoderite were obtained. Few experiments concerning the stability field of yoderite have been made thus far. Based on these earlier experiments, Schreyer (1988) presented a

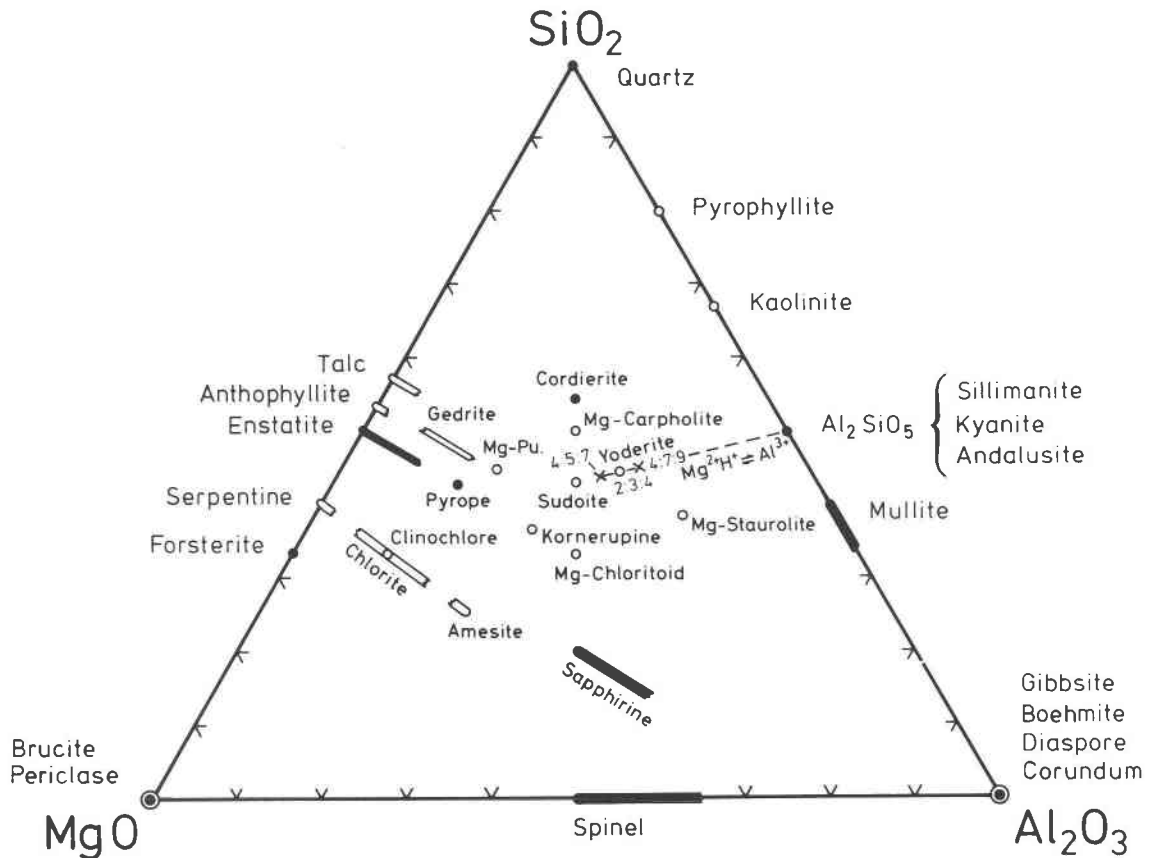


Fig. 1. Triangular plot of the system $\text{MgO-Al}_2\text{O}_3\text{-SiO}_2\text{-H}_2\text{O}$ (MASH) projected from H_2O , showing relevant phases and three possible compositions of hypothetical pure aluminum yoderite (numbers). Sudoite with the ratio 2:2:3 could be the projection point of an additional hypothetical yoderite composition. Note the substitution line $\text{Mg} + \text{H} = \text{Al}$, which in the projection lies between Al_2SiO_5 and forsterite. Mg-Pu = synthetic "MgMgAl-pumpellyite" (nomenclature of Schreyer, 1988). Open symbols are hydrous phases, solid symbols represent phases without essential H_2O .

possible stability field for yoderite in the MASH system lying in the range of 720–870 °C and at fluid pressures between 9 and 18 kbar.

In the unpublished work of Massonne and Schreyer, only two reactions resulting in the breakdown of yoderite toward lower temperatures ($\text{Yod} = \text{Chl} + \text{Ky} + \text{Tc}$) and lower pressures ($\text{Yod} = \text{Tc} + \text{Ky} + \text{Co}$) were studied experimentally, but the reaction rates were disappointingly low, even after experiment durations of 14 d (for mineral abbreviations see Table 1).

The aim of the present study was to monitor the influence of Fe^{3+} on the synthesis and stability of yoderite and to determine the Fe^{3+} contents of the synthetic products. We also investigated the influence of f_{O_2} on yoderite synthesis. It was hoped that the results would clarify the reasons that yoderite, a mineral consisting of only common elements, is known thus far to exist in only one locality in nature.

EXPERIMENTAL TECHNIQUES

All experiments were performed in a piston-cylinder apparatus of the type described by Boyd and England

(1960). The pressure cells, consisting of rock salt and fired pyrophyllite as solid state pressure media, involve negligibly small friction, so that pressure measurements have an accuracy of about 1% (Mirwald and Massonne, 1980). Steel tubes were used as resistance furnaces. The temperatures were measured by Ni-NiCr thermocouples with a range of uncertainty of ± 5 K. For equilibrium experiments, the temperatures were corrected for the temperature gradient in the high-pressure cell (Leistner, 1979). In all experiments, f_{O_2} was controlled by solid state buffers employing the technique described in detail by Eugster and Wones (1962). The outer capsule composed of Au contained the powdered buffer mixture, whereas the inner capsule consisting of Pd contained the charge. The outer capsule had the following dimensions: length = 16 mm, diameter = 6.1 mm, and wall thickness = 0.5 mm. For synthesizing yoderite, inner capsules with the following dimensions were used: length = 9 mm, diameter = 4.5 mm, and wall thickness = 0.25 mm. The equilibrium experiments were performed in Pd capsules that had a length of 6 mm and a diameter of only 2 mm. The absorption of Fe by Pd capsules from starting materials was

TABLE 1. Starting compositions and results of yoderite synthesis experiments

Gel no.	Gel I	Gel II	Gel III	Gel IV	Gel V	Gel VI	Gel VII	Gel VIII
Mol proportions								
MgO	2.0	2.0	2.0	2.0	2.0	2.0	2.0	2.0
Al ₂ O ₃	6.0	5.9999	5.999	5.99	5.95	5.9	5.8	5.6
Fe ₂ O ₃	—	0.0001	0.001	0.01	0.05	0.1	0.2	0.4
SiO ₂	4.0	4.0	4.0	4.0	4.0	4.0	4.0	4.0
Wt%								
MgO	12.86	12.86	12.86	12.86	12.84	12.81	12.75	12.63
Al ₂ O ₃	48.79	48.79	48.78	48.69	48.30	47.78	46.76	44.72
Fe ₂ O ₃	—	0.0013	0.013	0.13	0.64	1.27	2.52	5.00
SiO ₂	38.34	38.34	38.34	38.32	38.23	38.14	37.96	37.65
Phases obtained								
	En, Ky, St	Yod tr Co, En						
Wt%								
Chemical analyses of yoderite								
MgO		11.22	11.45	11.16	11.22	11.63	11.26	11.67
Al ₂ O ₃		48.56	48.61	50.02	47.30	47.47	47.47	46.33
Fe ₂ O ₃		0.14	0.10	0.23	1.03	1.34	2.63	4.47
SiO ₂		37.37	37.47	37.14	37.23	36.62	36.07	35.36
H ₂ O		2.70	2.68	2.70	2.72	2.63	2.32	2.63
Total		99.99	100.31	101.25	99.50	99.69	99.75	100.46
Atoms								
Structural formulae of yoderite								
Mg		1.79(7)	1.83(5)	1.77(4)	1.80(5)	1.88(3)	1.83(7)	1.89(9)
Al		6.14(9)	6.13(9)	6.26(9)	6.01(9)	6.06(3)	6.10(9)	5.94(9)
Fe		0.01(1)	0.01(1)	0.02(1)	0.08(2)	0.11(2)	0.21(3)	0.37(4)
Si		4.00(8)	4.01(7)	3.94(8)	4.01(7)	3.96(3)	3.93(6)	3.84(9)
H		1.93	1.91	1.88	1.97	1.90	1.70	1.91
Lattice parameters of yoderite								
a (Å)		7.9888(7)	7.9901(7)	7.9907(5)	7.9933(9)	7.9958(6)	7.9983(8)	8.0041(9)
b (Å)		5.7844(6)	5.7847(6)	5.7865(5)	5.7870(7)	5.7880(5)	5.7932(6)	5.8007(8)
c (Å)		7.2163(6)	7.2182(7)	7.2189(5)	7.2213(9)	7.2197(5)	7.2237(6)	7.2252(8)
β (°)		104.937(7)	104.889(9)	104.887(3)	104.974(9)	104.951(9)	104.925(7)	104.928(9)
V (Å ³)		322.20(4)	322.42(4)	322.58(4)	322.74(4)	322.81(3)	323.42(4)	324.15(5)

Note: Synthesis conditions were 880 °C, 15 kbar fluid pressure, 1–2 d, Mn₂O₃-MnO₂ buffer. Yoderite structural formulae are recalculated on the basis of 20 O atoms pfu. Abbreviations: Yod = yoderite, En = enstatite, Co = corundum, Chl = chlorite, Tc = talc, Hem = hematite, St = staurolite, Sill = sillimanite, tr = very small amounts barely detected by X-ray diffraction.

discussed by Stern and Wyllie (1975) and Muan (1976). For the relatively low temperatures and high f_{O_2} employed in this work, the absorption of Fe is negligible. The buffer used was, in most cases, a mixture of MnO₂ and Mn₂O₃ in the ratio of 3:1. In all cases, H₂O and intact buffer were present at the end of the experiments.

Gels were used as starting materials for all yoderite syntheses. They were prepared from Mg powder (Fluka AG, Switzerland), Al powder (Schuchardt, Munich), Fe plate (Johnson Matthey & Co. Ltd., London) and tetraethylorthosilicate (TEOS; Merck, Darmstadt). A list of the metal oxide proportions of the 12 gels used is given in Table 1. During the preparation of these Fe-bearing gels, the nitric acid oxidized metallic Fe into the trivalent state. The high f_{O_2} of the Mn₂O₃-MnO₂ buffer served to maintain this oxidation state throughout the experiments. The MnO₂ by J. T. Baker was used for the buffer. The second component, Mn₂O₃, was synthesized by heating MnO₂ for 2 d at 750 °C (Huebner and Sato, 1970).

The experiment samples, about 50 mg of gel plus 10 wt% added H₂O, were sealed in the Pd capsules. The excess H₂O (yoderite has an H₂O content of about 3%) was expected to accelerate the reaction. After the experiments, H₂O was also found in the inner capsules in all cases.

The synthetic products were identified by optical and X-ray techniques. Lattice parameters were calculated us-

ing an automatic powder X-ray diffractometer (Siemens) with a data reduction program (Diffrac 11); KI served as an internal standard.

In the equilibrium experiments, the trend of the reaction was determined by comparison of X-ray powder diffraction patterns of the starting mixture with those of the experimental products.

The chemical composition of all yoderite samples synthesized was determined with an automated electron microprobe (Camebax). The standards used were a glass of andradite composition, MgO, and Al₂O₃. The Fe analyzed was calculated as Fe₂O₃. H₂O analyses were performed with the Karl Fischer titration method (for details see Johannes and Schreyer, 1981).

Refractive indices were measured using the λ -T method. An oil with $n = 1.70$ (Cargille Laboratories Inc.) was used as the immersion medium. The method used is described in detail by Medenbach (1985). The reference crystal was smithsonite. Indexing of the crystal faces of synthetic yoderite was verified by the computer program SHAPE (Eric Dowty, Bogota, New Jersey 07603, U.S.A.).

EXPERIMENTAL RESULTS

Synthesis of yoderite

Because the composition of natural yoderite is very close to the composition 2:3:4 in the MASH system (Fig.

TABLE 1—Continued

Gel IX	Gel X	Gel XI	Gel XII
Starting compositions			
2.0	2.0	4.0	4.0
5.5	5.0	9.917	13.883
0.5	1.0	0.083	0.117
4.0	4.0	7.0	9.0
12.57	12.30	14.74	11.36
43.72	38.87	46.21	49.87
6.23	12.18	0.61	0.66
37.48	36.65	38.44	38.10
Phases obtained			
Yod tr Co, En Hem	Yod tr Co, En more Hem	Yod tr Co, En Chl	Yod tr Co, En
Chemical analyses of yoderite			
12.04	12.09	11.17	11.20
43.10	41.94	48.40	49.23
6.83	8.81	0.57	0.59
35.95	36.07	37.12	36.93
2.68	2.60	2.60	2.57
100.60	101.51	99.86	100.52
Structural formulae of yoderite			
1.96(5)	1.97(6)	1.82(7)	1.78(6)
5.56(9)	5.40(9)	6.18(9)	6.22(9)
0.56(3)	0.72(3)	0.04(1)	0.05(1)
3.93(7)	3.94(4)	3.95(9)	3.94(7)
1.97	1.90	1.84	1.83
Lattice paramters of yoderite			
8.0146(8)	8.0199(8)	7.9912(8)	7.9929(8)
5.8033(6)	5.8087(9)	5.7861(7)	5.7902(7)
7.2338(7)	7.2355(6)	7.2186(7)	7.2195(7)
104.940(9)	104.905(9)	104.905(9)	104.900(7)
325.08(4)	325.74(5)	322.54(4)	322.89(4)

1), we limited our main efforts to starting compositions with this oxide ratio. The compositions of two additional gels (4:5:7 and 4:7:9, Table 1 and Fig. 1) lie on both sides of the 2:3:4 composition, again along the connecting line between kyanite and forsterite. In order to determine the range of Fe³⁺ contents of synthetic yoderite, ten gels (I–X) with Fe³⁺ that is assumed to replace Al increasing from zero to 1.0 pfu were prepared (Table 1). The *PT* conditions for synthesis were chosen based on results of Schreyer and Yoder (1968). Table 1 shows also the results of phase analysis of the yoderite synthesis experiments.

With the exception of gel I, the Fe-free gel, and the most Fe-rich gels, the product phases detected by X-ray powder diffraction were, in all cases, yoderite plus very small amounts of enstatite and corundum. These three phases do not account for the total bulk composition of the starting materials (see Fig. 1), unless the synthetic yoderite samples have more (Al + Fe)-rich compositions than those of the starting gels. As will be shown later, this is indeed the case. Moreover, microprobe work on some of the experimental products has shown traces of Al₂SiO₅ as an additional phase. Schreyer and Seifert (1969) also failed to synthesize yoderite as a single-phase product. In addition to the above extra phases, hematite was a product of gels IX and X, the gels richest in Fe (0.5 and 1.0 Fe pfu). Most importantly, no yoderite whatsoever was obtained from gel I, which was absolutely free of Fe. On the

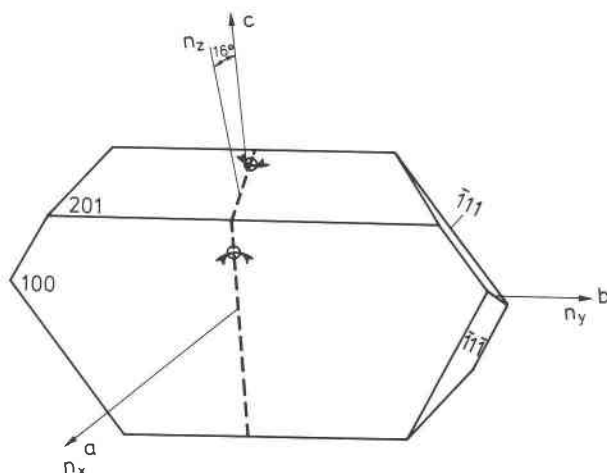


Fig. 2. Crystal morphology and orientation of optical indicatrix of synthetic yoderite containing 0.37 Fe per formula unit.

other hand, the trace amount of 0.0001 Fe pfu in gel II (= 0.0013 wt% of Fe₂O₃ in the starting gel) sufficed to stabilize yoderite. In a further attempt at synthesizing Fe-free yoderite at a different *P-T* condition, an experiment was carried out at 18 kbar and 800 °C with gel I, but the result was also negative, yielding enstatite + kyanite + staurolite, just as for the experiment at 15 kbar.

Physical properties of synthetic yoderite

The synthetic yoderite prepared from the Fe-bearing gels are mostly euhedral monoclinic, colorless, thin plates, usually with a maximum length of about 20 μm and a width of 5–10 μm. The thickness of the plates is estimated to be <5 μm. In order to obtain larger crystals for single-crystal studies, the duration of the experiments was extended up to 5 d. However, the results of these experiments showed that the Fe contents of gels have a stronger influence on crystal growth than does time. The less the Fe content, the smaller the size of the crystals. Euhedral yoderite crystals with a maximum length of about 100 μm were obtained only from gel VIII (0.4 Fe pfu). The morphology and the optical data were determined on one of these crystals (see Fig. 2). The yoderite sample prepared from gel VIII (0.4 Fe pfu, see Table 1) has the following optical data: *n_x* = 1.695(1), *n_y* = 1.696(1), *n_z* = 1.708(1), *n̄* = 1.700, Δ = 0.013, 2*V_z* = 47(1)°, and the optic axial plane is (010).

All reflections of the X-ray powder diffraction patterns of yoderite could be indexed on the basis of a monoclinic cell. The space group is *P2₁/m* or *P2₁* (Higgins et al., 1982).

The lattice parameters of synthetic Fe-bearing yoderite show the expected correlation with Fe contents (Fig. 3). Because of the larger ionic radius of trivalent Fe (0.705 Å) vs. Al (0.48 Å, values after Shannon, 1976), the cell parameters *a*, *b*, and *c* become larger with increasing Fe content, whereas β remains unaffected (Fig. 3). The relative influence of Fe is greatest along *b* and least along *c*

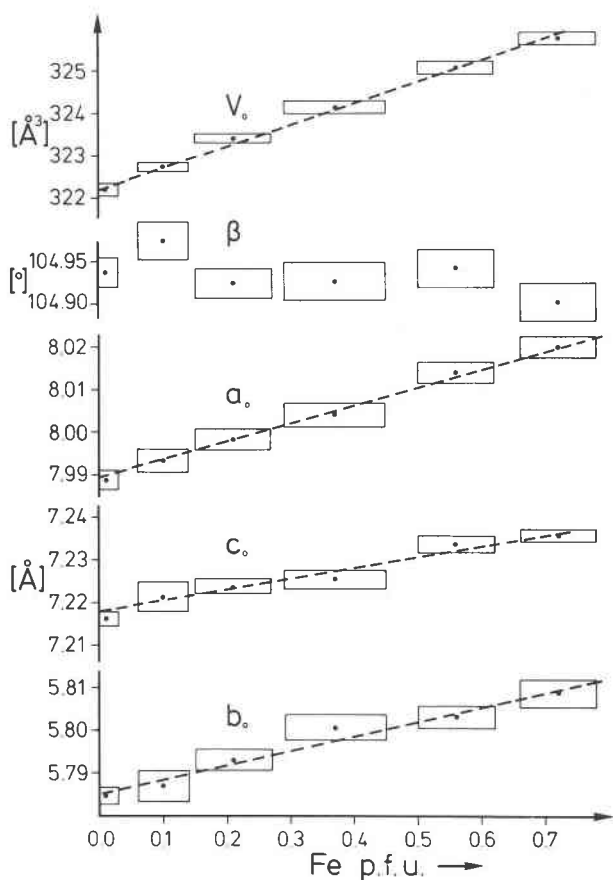


Fig. 3. Lattice parameters of synthetic yoderite as a function of Fe^{3+} content as determined analytically. For data see Table 1.

(Table 1). The equations for the correlation between Fe content and cell parameters are as follows: $a = 7.9897 + 0.0424 \cdot \text{Fe p.f.u.}$, $b = 5.7854 + 0.0336 \cdot \text{Fe p.f.u.}$, $c = 7.2180 + 0.0242 \cdot \text{Fe p.f.u.}$

The ordering problem of yoderite

In his single-crystal work on natural yoderite, McKie (1959) first described weak subsidiary reflections. Further investigations by Higgins et al. (1982) on a possible superstructure of yoderite showed that the Mg and Al ions are well ordered on the A(1) and A(2) positions, and possibly Al and Fe^{3+} are well ordered on A(3). This low-temperature structure changes on heating to 800 °C to one that is completely disordered. In the present work, we used the synthetic crystal shown in Figure 2 to obtain a zero-level, *b*-axis Weissenberg photograph. Since no satellite reflections were detected, it is likely that synthetic yoderite is disordered.

In addition, differential thermal analysis and thermogravimetric analysis of yoderite powder prepared from gel V (0.05 Fe p.f.u.) were recorded. With the exception of a strong exothermic peak at 950 °C, no further peaks occur. The one peak correlated with the dehydration of yoderite. However, McKie (1959) observed an additional endo-

thermic peak at about 500 °C, which he could not explain. The lack of a 500 °C peak for the probably disordered synthetic yoderite could indicate that this peak may somehow be related to initial stages of disorder in natural yoderite. Nonetheless, the apparent discrepancy between natural and synthetic yoderite in their Mg,Al and perhaps Al, Fe^{3+} ordering states requires further attention. Disorder in synthetic yoderite may be caused by the short experiment durations of only 5 d, but it may also be due to synthesis within a high-temperature stability field of disordered yoderite.

Chemical composition of synthetic yoderite

As mentioned before, synthetic yoderite was always associated with corundum and enstatite, and in two cases with additional hematite. These observations indicate that the compositions of synthetic yoderite cannot match those of the starting gels. In order to clarify this problem, microprobe and H_2O analyses from all synthetic materials were carried out. The results compiled in Table 1 indeed show remarkable deviations of the compositions of yoderite crystals from their starting gel compositions.

The analyzed Fe contents are, of course, of particular interest. Synthetic yoderite made from starting compositions with Fe contents of up to 0.4 Fe atoms pfu incorporate all the Fe present. Gels with more than 0.4 Fe atoms lead to the appearance of the excess phase hematite, although the coexisting yoderite exhibits Fe contents beyond 0.4 Fe pfu as well (Table 1). In the case of the most Fe-rich gel X (1.0 Fe atom pfu), the analyzed yoderite crystals have an Fe content of 0.72 Fe pfu. The observation that the yoderite crystals made from starting gel IX with 0.5 Fe pfu have an average Fe content of 0.56 Fe atoms pfu and that there is also some hematite, probably indicates overall disequilibrium.

In this connection, it was of interest to try to determine the maximum amount of Fe that can be incorporated stably into yoderite. Therefore, the experiments were continued for the products of yoderite synthesis obtained from gel X (Table 1) at the same *PT* conditions for two more days. The comparison of the lattice parameters of yoderite before and after the experiment show a decrease of the Fe content of yoderite from 0.72 to 0.65 Fe pfu. This observation indicates that yoderite with an Fe content of 0.72 pfu is metastable for these experimental conditions. The value of 0.4 Fe pfu in natural yoderite coexisting with hematite might suggest that the stable limit for Fe incorporation into yoderite lies near 0.4 pfu, although it may, of course, vary with pressure, temperature, and f_{O_2} .

The Mg contents of all analyzed yoderite samples are considerably lower than 2.0 Mg atoms pfu; however, yoderite incorporates more than 6.0 atoms of (Al + Fe^{3+}) in its crystal structure. The analyzed H_2O content is lower than 2.0 (OH) groups pfu, and the Si content generally deviates very slightly from the ideal formula to lower values. The deviations of the Mg : (Al,Fe) : Si ratios of the crystals from the starting compositions are summarized statistically by the following two equations:

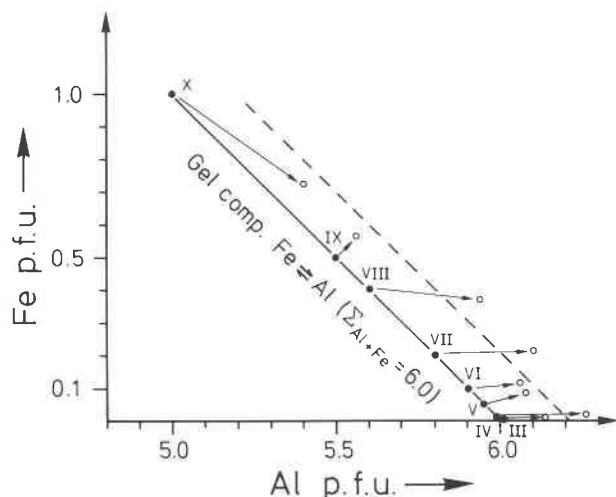
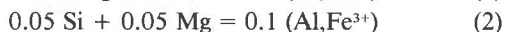


Fig. 4. Plot of the analyzed Al and Fe contents of synthetic yoderite (open circles) compared with those of its starting gels (solid dots; Roman numerals define the gels as in Table 1). Arrows connect gels and products.



Equation 1 is the substitution assumed for yoderite to lie along the join kyanite-forsterite, and Equation 2 is, of course, the well-known Tschermak substitution.

Figure 4 depicts graphically the relationship of the Al and Fe³⁺ contents in the starting gels vs. those of the analyzed yoderite. The analytical points of yoderite consistently plot to the right of the theoretical substitution line Fe = Al, especially at low Fe contents. The offset of points for the analytical data is a result of deviations from the ideal formula Mg₂(Al,Fe³⁺)₆Si₄O₁₈(OH)₂ owing to substitutions 1 and 2. The arrows indicate the degree of Fe incorporation in yoderite, as discussed above.

In a still more informative plot, Figure 5 shows the Al-Fe fractionation, if any, between the starting gel and the synthetic yoderite. Intermediate compositions (gels IV–IX and XI, with Fe 0.01–0.5) incorporate practically all of the Fe present in the gel; the deviation of the gel V product is due to strong heterogeneity between individual crystals. Very Fe-poor compositions (gels II and III) give rise to fractionation of Fe strongly into yoderite by factors of up to 100, although the microprobe analytical errors for such small amounts of Fe may be particularly high. On the Fe-rich side, there is an opposite trend caused by the limiting capacity of yoderite for Fe at these experimental conditions.

Another interesting feature is the positive correlation between the Fe and Mg contents in the yoderite samples synthesized (Fig. 6). Larger Fe³⁺ contents are correlated with enhanced Mg contents, as consistent with the radii of both Fe³⁺ and Mg being greater than the radius of Al. Thus the Mg value of 2.0 of the ideal formula is approached by the most ferric yoderite samples.

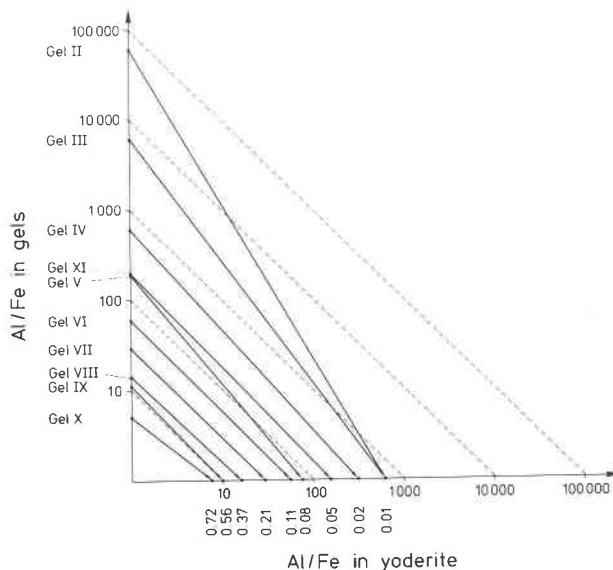


Fig. 5. Comparison between the Al-Fe ratios of starting gels (Roman numerals as in Table 1) and those of the resultant yoderite products. Note fractionation of Fe into yoderite at high Al-Fe and the opposite trend at low Al-Fe, when hematite appears as an excess phase. Numbers at bottom indicate the analyzed Fe contents pfu in yoderite (Table 1). Thin broken lines indicate no fractionation. For discussion of differences in gel V products see text.

Answers to these mineral chemical problems require data on the true cation occupancies of the polyhedra in synthetic yoderite.

The high values of the standard deviations of the calculated cation contents of yoderite (Table 1) indicate again that the chemical compositions of the yoderite grains in one sample are heterogeneous. Given the relatively short duration of the synthesis experiments, this heterogeneity is not surprising.

Preliminary PTX-stability experiments

It was mentioned in the previous section that yoderite with Fe contents higher than about 0.4–0.5 pfu may be metastable for the synthesis conditions chosen here. In this section, we report on experiments that shed light on the minimum Fe content that is required by the crystal structure to stabilize yoderite.

Schreyer (1988) presented a possible stability field for a hypothetical pure magnesium aluminum yoderite at temperatures between 700 °C and 870 °C with fluid pressures of 9 and 18 kbar. The breakdown reactions toward lower temperatures and lower pressures were studied experimentally by Massonne and Schreyer (unpublished work) using crystalline phases obtained from an Fe-free starting mixture. However, there were small amounts of Fe present because the starting material was seeded twice with natural Fe-bearing yoderite from Tanzania.

In this work, the amount of Fe necessary for nucleation and growth of yoderite in synthesis experiments was

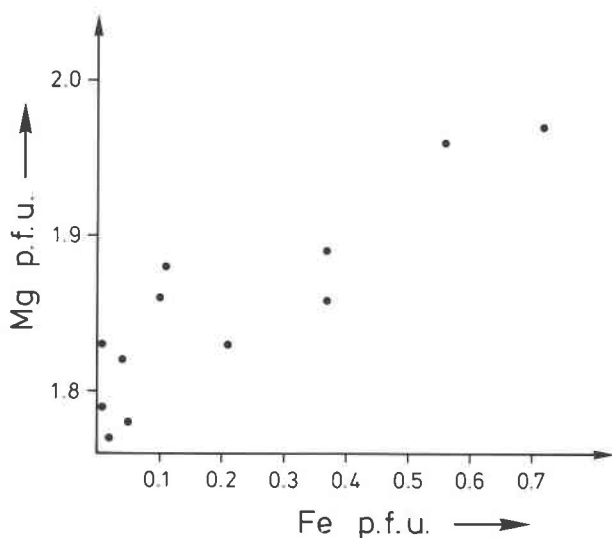


Fig. 6. Plot of analytical Mg and Fe contents per formula unit of synthetic yoderite. Note the positive correlation.

extremely small (see Table 1). In order to test such very Fe-poor yoderite for its true thermodynamic stability, seeding experiments are necessary using—in separate experiments—all theoretically possible alternative assemblages.

In this study, we concentrated on one alternative assemblage that is given in Figure 7 of Schreyer (1988) as one possible high-temperature breakdown product of yoderite: enstatite + staurolite + kyanite. This assemblage was prepared in our work at 800 °C and 25 kbar with a Mn_2O_3 - MnO_2 buffer, from four different gels (III, V, VII, VIII) also used for yoderite synthesis (see Table 1 for their compositions). The products were seeded with the requisite yoderite crystals (prepared previously from these gels) and sealed in small Pd capsules with about 10 wt% excess H_2O . Experiments were carried out 750 °C and 10 kbar for 3 d, again employing the Mn_2O_3 - MnO_2 buffer. The PT values chosen lie well within the yoderite field as proposed by Schreyer (1988).

TABLE 2. Experimental data on the stability of yoderite as a function of Fe content

Starting gel no.	Fe pfu	Relative amount of yoderite	Relative amount of St + En + Ky
III	0.001	decreases	increases
V	0.1	decreases	increases
VII	0.2	increases	decreases
VIII	0.4	increases	decreases

Note: Starting mixtures consisted of yoderite with various compositions (for these and for synthesis conditions see Table 1), with the alternative assemblage St + En + Ky (obtained at 25 kbar, 800 °C, 1 d from the requisite gels plus 10 wt% H_2O added. Conditions for the equilibrium experiments were 10 kbar, 750 °C, 3 d. Buffering in all cases with Mn_2O_3 - MnO_2 .

TABLE 3. Synthesis experiments for Fe-bearing yoderite employing various buffers

Buffer	Phases obtained
Mn_3O_4 - Mn_2O_3	Yod, tr En, Co
Fe_3O_4 - Fe_2O_3	Yod, St (2%), tr En
Ni-NiO	Yod, St (5%), tr En
$Fe_{1-x}O$ - Fe_3O_4	Yod, St (10%), tr En
No buffer	Yod, St (30%), tr En, Sill(?)

Note: Starting material: gel VIII with 0.4 Fe pfu. Experimental conditions: 15 kbar, 800 °C, 2 d. Abbreviations: see Table 1.

The results listed in Table 2 imply breakdown of the Fe-poor yoderite crystals and growth of more Fe-rich ones. We interpret this as an indication of the instability of yoderite with Fe contents of less than approximately 0.2 pfu at these PT conditions.

The distribution of Fe^{3+} in the phases in the assemblage staurolite + kyanite + enstatite is not yet resolved. Hematite was not observed as an excess phase. Thus, it is suspected that Fe is mostly incorporated in staurolite, but the other phases may contain small amounts of Fe^{3+} as well. Kyanite, for example, may have approximately 0.13 Fe^{3+} per 5 O atoms (Langer and Frentrup, 1973).

Obviously, these results represent only a very first approximation to the problem of PTX stability relations of yoderite. With Fe^{3+} being a necessary and variable component in yoderite, the PT field published by Schreyer (1988) may have to be modified in many respects.

Experiments with various oxygen fugacities

The influence of different f_{O_2} on the synthesis of yoderite was tested using other O buffers. A list of the buffers used and the experimental products obtained is given in Table 3. All of these experiments were performed with the same starting gel at the same PT conditions which had proved to be best for yoderite synthesis.

The results show that yoderite crystallized under a wide range of f_{O_2} with and without a buffer. However, contrary to the experiments with the Mn_2O_3 - MnO_2 buffer, the excess phase staurolite appeared, rather than corundum, and increased in amount as f_{O_2} decreased. These results may be explained as follows: all of the Fe in the gel is in the trivalent state as a result of the oxidizing influence of nitric acid during gel preparation. Thus, the initial nucleation of yoderite is favored relative to that of other phases. During the experiment, however, the buffer caused f_{O_2} to decrease, thus reducing the Fe to the ferrous state. If yoderite cannot incorporate Fe^{2+} , it breaks down and forms another Fe^{2+} phase, namely staurolite.

Although equilibrium experiments with precrystallized starting materials are necessary for compelling evidence, we conclude from these preliminary synthesis data that very high f_{O_2} are required in order to nucleate yoderite and to retain it as a stable phase both in experiments and nature. Yoderite is considered to be a stable phase under the f_{O_2} conditions of the Mn_2O_3 - MnO_2 and Mn_3O_4 - Mn_2O_3 buffers.

DISCUSSION

The experimental results reported here indicate that yoderite requires a finite minimum amount of Fe^{3+} to become a stable mineral phase, but also has a rather limited capacity for this component. Both features are probably governed by its crystal structure, in which the five-coordinated A(3) site should be slightly larger than when only occupied by Al (Ungaretti, personal communication).

The limited composition range of yoderite, as found in this study, has interesting petrological applications and consequences. Figure 7 shows the approximate extension of yoderite solid solution in the system $\text{MgO-Al}_2\text{O}_3\text{-Fe}_2\text{O}_3\text{-SiO}_2\text{-H}_2\text{O}$ (MAFSH) projected from $\text{SiO}_2 + \text{H}_2\text{O}$ onto the MAF plane. Although the conditions for the coexistence of yoderite with quartz have yet to be elaborated on by further experimentation, the Tanzania yoderite schist presents evidence that this assemblage is stable for given conditions of PT and f_{O_2} , which are as yet unknown. The theoretical compatibility relations, as shown in Figure 7, imply that only yoderite in the assemblage with talc and hematite (+ quartz) can exhibit the maximum Fe content, whereas this is not so for the assemblage with kyanite and hematite (+ quartz). Indeed, as McKie (1959) has pointed out, kyanite is always found to be surrounded by yoderite in the Mautia Hill rock, and therefore could not exist in the fully reacted stable assemblage. In accordance with these phase relations, in Figure 7 the projection point of the whole-rock composition of the yoderite schist as reported by McKie (1959) falls into the field $\text{Tc} + \text{Yod} + \text{Hem}$ (+ Qz). Thus, the yoderite-forming reaction at Mautia Hill must actually have been talc + kyanite + hematite = yoderite + quartz.

Yoderite with minimum Fe^{3+} contents can be expected only in rocks rather poor in Fe_2O_3 , giving rise to the hematite-free assemblage yoderite + kyanite + talc + quartz (lowermost part of Fig. 7). It might be worthwhile to search in the Mautia Hill schists for such local environments with yoderite of different compositions.

Concerning further experimental work on yoderite, there are, of course, still many unresolved problems. Certainly of foremost importance are data on the true $PTXf_{\text{O}_2}$ stability field of yoderite as a function of PTX and f_{O_2} and its limits toward lower and higher fluid pressures, as well as lower and higher temperatures. All of these relations are again open for discussion relative to the diagram of Schreyer (1988). Furthermore, the compatibility of yoderite with quartz and definition of its PTX relations may lead to a better understanding of the petrogenesis of the Tanzania yoderite schist. As yoderite is still only known to occur at Mautia Hill, the problem of its uniqueness must be considered further. The solution proposed by Schreyer and Yoder (1968) in which they attributed this uniqueness to a very small PT field for the pair yoderite + quartz, does not seem valid in light of the present data. Experimentation directed toward solving at least some of these problems is presently under way at Bochum.

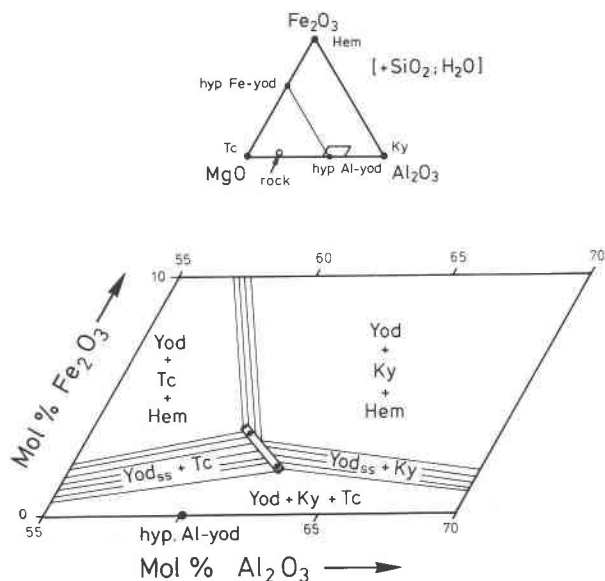


Fig. 7. Projection of the MAFSH system onto the silica- and H_2O -free base plane (triangle above) showing the locations of the phases talc (Tc), kyanite (Ky), and hematite (Hem) as well as the hypothetical yoderite solid solution line $\text{Mg}_2\text{Al}_6\text{Si}_4\text{O}_{18}(\text{OH})_2\text{-Mg}_2\text{Fe}_6\text{Si}_4\text{O}_{18}(\text{OH})_2$. The open circle represents the projection point of the bulk yoderite schist from Mautia Hill, Tanzania, as reported by McKie (1959). The enlarged portion in the lower figure shows the true range of yoderite compositions, as derived from the present work, and the expected tie line bundles toward Tc, Ky, and Hem in the presence of excess quartz. Small solid dots are the projection points of microprobe analyses of synthetic yoderite with 0.21 and 0.37 Fe pfu (see Table 1).

ACKNOWLEDGMENTS

This paper represents part of the Diploma thesis of the senior author, completed at Ruhr-Universität Bochum in early 1989.

The authors want to thank several people at the Bochum Institute, especially M. Lehmann, who drafted the diagrams, G. Andersen and Th. Baller for their help in conducting the experiments, and O. Medenbach for determining the optical data of yoderite. We are also grateful to L. Ungaretti in Pavia for stimulating discussions on the crystal chemistry of yoderite. The manuscript was reviewed by W.D. Carlson, J.B. Higgins, and H.S. Yoder, Jr.

REFERENCES CITED

- Boyd, F.R., and England, J.L. (1960) Apparatus for phase-equilibrium measurements at pressures up to 50 kbars and temperatures up to 1750 °C. *Journal of Geophysical Research*, 65, 741–748.
- Eugster, H.P., and Wones, D.R. (1962) Stability relations of the ferruginous biotite, annite. *Journal of Petrology*, 3, 82–125.
- Fleet, S.G., and Megaw, H.D. (1962) The crystal structure of yoderite. *Acta Crystallographica*, 15, 721–728.
- Higgins, J.B., Ribbe, P.H., and Nakajima, Y. (1982) An ordering model for the commensurate antiphase structure of yoderite. *American Mineralogist*, 67, 76–84.
- Huebner, J.S., and Sato, M. (1970) The oxygen fugacity–temperature relationships of manganese and nickel oxide buffers. *American Mineralogist*, 55, 934–952.
- Johannes, W., and Schreyer, W. (1981) Experimental introduction of CO_2 and H_2O in cordierite. *American Journal of Science*, 281, 299–317.
- Langer K., and Frentrup K.P. (1973) Synthesis and some properties of

- iron- and vanadium-bearing kyanites, $(\text{Al}, \text{Fe}^{3+})_2\text{SiO}_5$ and $(\text{Al}, \text{V}^{3+})_2\text{SiO}_5$. *Contributions to Mineralogy and Petrology*, 41, 31–46.
- Leistner, H. (1979) Temperaturgradienten-Messungen in Piston-Zylinder Pressen. *Fortschritte der Mineralogie*, 57, 81–82.
- McKie, D. (1959) Yoderite, a new hydrous magnesium iron aluminosilicate from Mautia Hill, Tanganyika. *Mineralogical Magazine*, 32, 282–307.
- McKie, D., and Bradshaw, N. (1966) A green variety of yoderite. *Nature*, 210, 1148.
- Medenbach, O. (1985) A new microrefractometer spindle-stage and its application. *Fortschritte der Mineralogie*, 63, 111–133.
- Mirwald, P.W., and Massonne, H.-J. (1980) Quartz = coesite transition and the comparative friction measurements in piston-cylinder apparatus using talc-alsimag-glass (TAG) and NaCl high pressure cells: A discussion. *Neues Jahrbuch für Mineralogie Monatshefte*, 10, 469–477.
- Mruma, A.H., and Basu, N.K. (1987) Petrology of the talc-kyanite-yoderite schist with associated rocks of Mautia Hill, Mpwapwa District, Tanzania. *Journal of African Earth Sciences*, 6, 301–311.
- Muan, A. (1976) Mineral equilibria in an interdisciplinary perspective. *American Mineralogist*, 61, 355–365.
- Schreyer, W. (1988) Experimental studies on metamorphism of crustal rocks under mantle pressures. *Mineralogical Magazine*, 52, 1–26.
- Schreyer, W., and Schairer, F. (1961) Compositions and structural states of anhydrous Mg-cordierites: A reinvestigation of the central part of the system $\text{MgO}-\text{Al}_2\text{O}_3-\text{SiO}_2$. *Journal of Petrology*, 2, 324–406.
- Schreyer, W., and Seifert, F. (1969) High-pressure phases in the system $\text{MgO}-\text{Al}_2\text{O}_3-\text{SiO}_2-\text{H}_2\text{O}$. *American Journal of Science*, 267-A, 407–443.
- Schreyer, W., and Yoder, H.S., Jr. (1968) Yoderite: Synthesis, stability, and interpretation of its natural occurrence. *Carnegie Institution of Washington Year Book*, 66, 376–380.
- Shannon, R.D. (1976) Revised effective ionic radii and systematic studies of interatomic distances in halides and chalcogenides. *Acta Crystallographica*, A 32, 751–767.
- Stern, C.R., and Wyllie, P.J. (1975) Effect of iron absorption by noble-metal capsules on phase boundaries in rock-melting experiments at 30 kilobars. *American Mineralogist*, 60, 681–689.

MANUSCRIPT RECEIVED JANUARY 24, 1990

MANUSCRIPT ACCEPTED FEBRUARY 13, 1991